

Supporting Information

Goudemand et al. 10.1073/pnas.1101754108

SI Methods

Propagation Phase-Contrast X-Ray Synchrotron Microtomography.

The specimens were scanned at the European Synchrotron Radiation Facility (ESRF) on the beamline ID19. We used a pink beam with a critical energy of 17.68 keV delivered by a U17.6 undulator. This insertion device delivers a single harmonic with a narrow bandwidth ($\Delta E/E$ of 5%). The original source monochromaticity is good enough to perform high-quality scans at submicron resolution without a monochromator. It allows rapid scans of microfossils, nearly free of ring artifacts. Regarding the sample size, we used a detector composed of a 6- μm thick GGG scintillator, of a revolver microscope, and of a FReLoN CCD camera (1). The isotropic voxel sizes ranged from 0.23 to 0.46 microns. Phase contrast was obtained using a propagation distance of 10 mm. Because absorption contrast is often low in fossils, phase contrast can reveal much more in structures (2–4).

1. Labiche JC, et al. (2007) Invited article: The fast readout low noise camera as a versatile x-ray detector for time resolved dispersive extended x-ray absorption fine structure and diffraction studies of dynamic problems in materials science, chemistry, and catalysis. *Rev Sci Instrum* 78:091301.
2. Tafforeau P, et al. (2006) Applications of X-ray synchrotron microtomography for non-destructive 3D studies of paleontological specimens. *Appl Phys. A* 83:195–202.

Processing of Raw Data. Radiographs were processed using in-house tools developed at the ESRF. They were corrected by flatfield and darkfield, using a protocol that reduces ring artifacts. Sample movements were measured and corrected later during the tomographic reconstruction. An average of the processed radiographs was computed and filtered to obtain a correction map for ring artifacts. The volumes were then reconstructed using a filtered back-projection algorithm (PyHST, ESRF). After reconstruction, the remaining ring artifacts were corrected slice by slice. The final slices were converted into stacks of 16-bit TIFF files for the 3D processing.

3D Processing. The 3D model was constructed using both the commercially available Amira imaging software and the in-house software FoRM-IT, developed by Christoph Zollikofer (University of Zurich).

All of the synchrotron data presented in this paper are available on the open access paleontological database of the ESRF at <http://paleo.esrf.eu>.

3. Feist M, Liu J, Tafforeau P (2005) New insights into Paleozoic charophyte morphology and phylogeny. *Am J Bot* 92:1152–1160.
4. Friis EM, et al. (2007) Phase-contrast X-ray microtomography links Cretaceous seeds with Gnetales and Bennettitales. *Nature* 450:549–552.

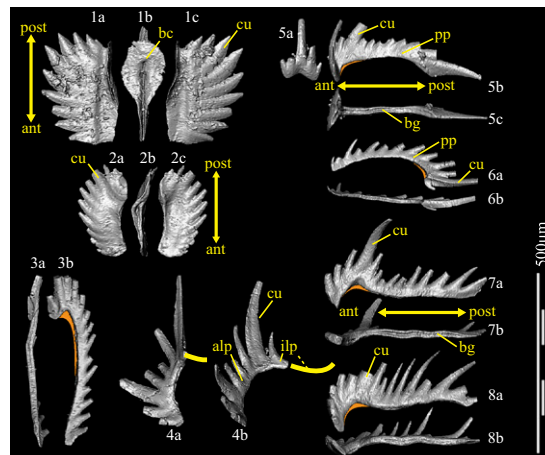
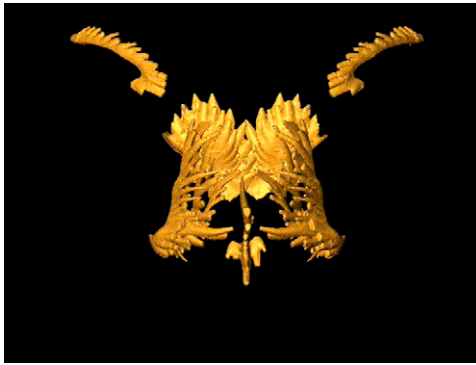


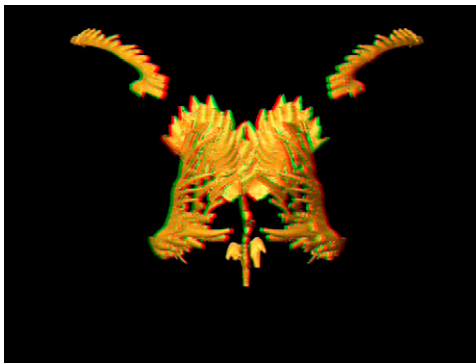
Fig. S1. “Standard” orientation of the single elements of *Novispathodus*. The pit of the basal cavity (bc) corresponds to the growth center. The denticle directly above this growth center is called the cusp (cu). Per definition, the cusp is curved toward the posterior end of the element. ant: anterior; post: posterior; alp: antero-lateral process; ilp: inner-lateral process; pp: posterior process; bg: basal groove. (1, a–c) P1. (2, a–c) P2. (3, a and b) M. (4, a and b) S2: the common extension of the broken inner-lateral process is indicated in yellow (1). (5, a–c) S0. (6, a and b) S1. (7, a and b) S3. (8, a and b) S4. The light orange area below the cusp of each ramiform element (3 and 5–8) shows the hypothesized potential extension of the basal body.

1. Orchard MJ (2005) Multielement conodont apparatuses of Triassic Gondolelloidea. *Conodont Biology and Phylogeny: Interpreting the Fossil Record*, eds. Purnell MA, Donoghue PCJ (*Spec Pap Palaeontol*), Vol 73, pp. 73–101.



Movie S1. Animated reconstruction of the feeding apparatus of conodont *Novispathodus*. In the protracted (opened) arrangement of the apparatus, S_3 and S_4 elements can close and grasp the prey. S_{2-4} elements start to retract and pull on the prey's tissues while the symmetrical S_0 and the M elements come to close in an opposing, Y-shaped converging motion. The S_0 and S_1 then retract caudally, tear off the seized tissues, and bring them toward the cutting/shearing P elements. The accompanying closure of the S_{2-4} elements helps to channel the food. Especially in lateral and caudal views, it is clear that all S elements rotate about a subcylindrical, presumably cartilaginous support: the inferred lingual (apical) cartilage.

[Movie S1](#)



Movie S2. Three-dimensional animated reconstruction of the feeding apparatus of conodont *Novispathodus*, a red/cyan anaglyph (3D) version of [Movie S1](#). Please use appropriate glasses.

[Movie S2](#)